Mechatronics 32 (2015) 12–21

Contents lists available at ScienceDirect

Mechatronics

journal homepage: www.elsevier.com/locate/mechatronics

Technical note

A foot-wearable interface for locomotion mode recognition based on discrete contact force distribution

Baojun Chen [a], Xuegang Wang [a], Yan Huang [a, c], Kunlin Wei [b], Qining Wang [a, *]

[a] The Robotics Research Group, College of Engineering, Peking University, Beijing 100871, China
[b] Motion Control Laboratory, Department of Psychology, Peking University, Beijing 100871, China
[c] Key Laboratory of Biomimetic Robots and Systems, Ministry of Education, Beijing Institute of Technology, Beijing 100081, China

ARTICLE INFO

Article history:
Received 24 October 2014
Accepted 6 September 2015
Available online 1 October 2015

Keywords:
Wearable sensing
Contact force
Locomotion mode recognition
Human–machine interface
Robotic assistive device

ABSTRACT

The knowledge of plantar pressure distribution is important in understanding human locomotion activities, and its integration with robotic assistive devices is an important potential application. In this paper, we aim to explore the potential of using discrete contact force distribution signals for locomotion mode recognition. A foot-wearable interface comprising a pair of sensing insoles, each with four sensors at selected locations, has been designed to record discrete contact forces during locomotion. Based on the information of discrete contact force distribution, we present a locomotion mode recognition strategy with decision tree and linear discriminant analysis classifiers. To verify the measurement performance of the sensing system, experiments are carried out to investigate the system stability in long term working conditions and its adaptation to different ground surfaces. To evaluate whether discrete contact force signals can be used for locomotion mode recognition, five able-bodied subjects and one amputee subject are recruited and asked to perform six types of locomotion tasks. With the proposed recognition strategy, reliable recognition performance is obtained. The average classification accuracy is 98.8% ± 0.5% for able-bodied subjects and 98.4% for the amputee subject, which is comparable to those obtained from systems based on other sensors. These experimental results indicate that monitoring of discrete contact force distribution is valuable for locomotion mode recognition. Its use can be combined with other sensing systems to achieve better performance of locomotion mode recognition for intelligent assistive device control.

1. Introduction

Plantar pressure distribution reveals detailed information about foot contact, which is of great value for human gait analysis. Compared with platform based measurement systems (e.g. force plate), wearable contact force sensing systems (e.g. in-shoe sensors) are more portable and convenient for long-term measurement of daily activities, especially in outdoor environments. They allow wider applications with respect to abnormal gait analysis, footwear design, and terrain performance [1]. Various commercial products such as F-Scan® by Tekscan [2], Pedar® by Novel [3] and prototypes of foot wearable measurement systems [1,4–13] have been proposed with various applications in sports and gait monitoring. Though wearable plantar pressure measurement systems have already been applied in many fields, there are still potential application spaces in other areas.

One possible application of wearable contact force measurement systems is its integration with robotic assistive devices, e.g. powered lower-limb prostheses. Most current locomotion assistive robots are controlled by finite state machine (FSM) models. Each locomotion mode (e.g. level-walking and stair ascent) has its own control strategy. To better assist humans and achieve natural gait patterns with less energy consumption, these advanced assistive devices should first "know" human movement intentions and then select the appropriate control mode [14–16]. Therefore, locomotion mode recognition is an important issue for robotic assistive device control. Signals used for locomotion mode recognition can be roughly divided into two main categories. The first category includes bioelectric signals related to human movement, with electromyography (EMG) being the most widely used for locomotion mode recognition [17–19]. Huang et al. proposed a phase-dependent recognition system to recognize seven locomotion modes using surface EMG signals of lower-limb muscles. The average classification accuracy was 92.2% for able-bodied subjects and 91.6% for amputee subjects. Human body capacitance sensing, which detects leg shape changes caused by

* Corresponding author. Tel./fax: +86 10 6276 9138.
E-mail address: qiningwang@pku.edu.cn (Q. Wang).

http://dx.doi.org/10.1016/j.mechatronics.2015.09.002
0957-4158/

muscle contractions during locomotive movements, provides another signal for movement recognition with comparable accuracy [20,21]. In [21], 10 channels of capacitance signals measured from the lower limb were used to recognize six locomotion tasks. Average recognition accuracies for able-bodied subjects and amputee subjects were 93.6% and 93.4%, respectively. However, for both EMG and capacitance signal measurement, electrodes should directly contact skin, which may cause inconvenience and discomfort. The other kind of sensors used for locomotion mode recognition are on-board mechanical sensors, which includes gyroscopes, accelerometers, goniometers and magnetometers [22–24]. Varol et al. presented a real-time recognition approach based on prosthesis-implemented sensors. Signals measuring joint angles and angular velocities of the knee and ankle, socket sagittal plane moment, foot forces of heel and ball were collected to realize the recognition of three locomotion modes (standing, sitting, and walking) and transitions between them [22]. However, these signals usually vary with accumulated errors or time-related drifts. To realize satisfactory and reliable recognition performance, classification methods based on multi-sensor fusion were developed in recent years. Huang et al. proposed an EMG-mechanical fusion approach, and obtained much better recognition performance than using only mechanical or EMG signals [25]. Therefore, it is meaningful to add more useful movement information to existing locomotion mode recognition systems in order to further improve the performance. Plantar pressure distribution contains rich information on human gait. However, most existing prosthesis-implemented and orthosis-implemented contact force measurement systems are only used for the detection of gait events or gait phases [26–31]. To our knowledge, no previous studies have investigated whether the information of contact force can be used to recognize multiple locomotion tasks (e.g. standing, level-ground walking, stair ascent, and stair descent) for robotic assistive device control.

In this paper, we explore the potential of using plantar pressure distribution information for human locomotion mode recognition. To make a systematical analysis, we design a foot-wearable interface, which is comprised of a pair of sensing insoles and transmission circuits. Each of the sensing insoles is integrated with four force sensors to measure discrete contact force distribution signals. To evaluate whether discrete contact force signals can be used for locomotion mode recognition, we propose a classification strategy based on decision tree analysis and linear discriminant analysis, and off-line recognition analysis is performed. To verify the measurement performance of the proposed system, experiments are carried out to investigate system stability of long term working on and adaptability to different ground surfaces. Five able-bodied subjects and one transtibial amputee subject are recruited and asked to perform six types of locomotion tasks, which include sitting, standing, walking, obstacle clearance, stair ascent, and stair descent. Satisfactory recognition performances are obtained for both able-bodied subjects and the amputee subject. These results indicate that discrete contact force distribution signals do provide valuable information for human locomotion mode recognition, and the proposed system can be combined with existing recognition systems based on other sensing information to obtain better recognition performance.

The rest of this paper is organized as follows. Section 2 describes the measurement system in detail. Section 3 presents the locomotion mode recognition strategy. Experiments and results are described in Section 4. The conclusion is made in Section 5.

2. Discrete contact force distribution measurement system

We presented a foot-wearable interface for locomotion mode recognition based on discrete contact force distribution. The interface was composed of a pair of sensing insoles, signal process circuit modules, and a base station connected to a host computer (Fig. 1(a)). Discrete contact force distribution is measured by sensing insoles placed in users' shoes. The signal processing module transmits signals to the base station via wireless. The base station rearranges signal sequences measured from different feet, and then transmits the data to the host computer.

Force sensors placed on sensing insoles are used to measure discrete contact force distribution. To fit users with differently sized feet, sensing insoles with different sizes are prepared in advance.

2.1. Sensing insole

2.1.1. Sensor placement

Though plantar pressure distribution of the whole foot contains richer information, discrete contact force distribution might be enough to investigate certain foot functions during walking and other locomotion activities [32]. To collect sufficient information for locomotion mode recognition with fewer force sensors, properties of plantar pressure distribution are analyzed to guide the placement of force sensors.

In this research, the method used for investigating contact forces of different foot sole zones is similar to the one used in our previous work [33]. Plantar pressure distribution of the whole foot is measured with a force plate, *footscan® advanced & hi-end system* (RSscan, Inc.,). The plate is 2 m × 0.4 m in size, with a sensor density of about $2.7 \times 10^4/m^2$. Each sensor embedded in the plate has a size of 0.005 m (lateral) × 0.007 m (anterior–posterior). Three able-bodied subjects and one unilateral transtibial amputee subject (left side amputated) were asked to walk on the plate without wearing shoes. The amputee subject walked with his own prosthetic foot (Otto bock 1S90). Contact force distribution of each step was measured by the plate automatically, and the sampling rate was 250 Hz. In this experiment, each subject was required to walk through the force plate for 5 times. The entire plantar pressure distribution area was divided into 10 zones (Fig. 2(a)). Fig. 2(b)–(e) shows the contact force distribution of the amputee subject and one of the able-bodied subjects. We can notice that the contact force distribution of the prosthetic foot is not exactly the same as the intact foot, probably due to the absence of ankle and toe joints. However, contact force distributions of prosthetic feet and intact feet might share common biomechanical characteristics.

Contact force distribution data of each zone within each step were calculated for each subject, and principal component analysis (PCA) was performed. Results showed that the variance ratio contributions of the first two principal components for all the subjects were above 90%. Then the absolute values of the loading coefficients of different zones in the first two principal components were compared, and *Z 1, 6, 9, 8* were found as the four largest when compared overall. These four zones made more contributions than the other zones in the first two principal components.

Thus, we selected these four zones as the positions for sensor placement. The four zones were defined as follows: (a) under the calcaneus tuberosity (*Z 1*); (b) under the fourth metatarsal (*Z 6*); (c) under the first metatarsal (*Z 8*); and (d) under the hallux (*Z 9*). However, the shape of an insole is not exactly the same as human foot. The positions of force sensors on an insole were empirically determined (Fig. 1(b)).

2.1.2. Force sensors

When the foot-wearable measurement system is used during walking, subjects do not expect to feel any discomfort. Therefore, the size, thickness and transmission model should be considered for force sensor selection. The size of the force sensor is limited by the size of the foot. A coin-size force sensor would be appropriate, as its contact region is large enough to guarantee quality signal measurement

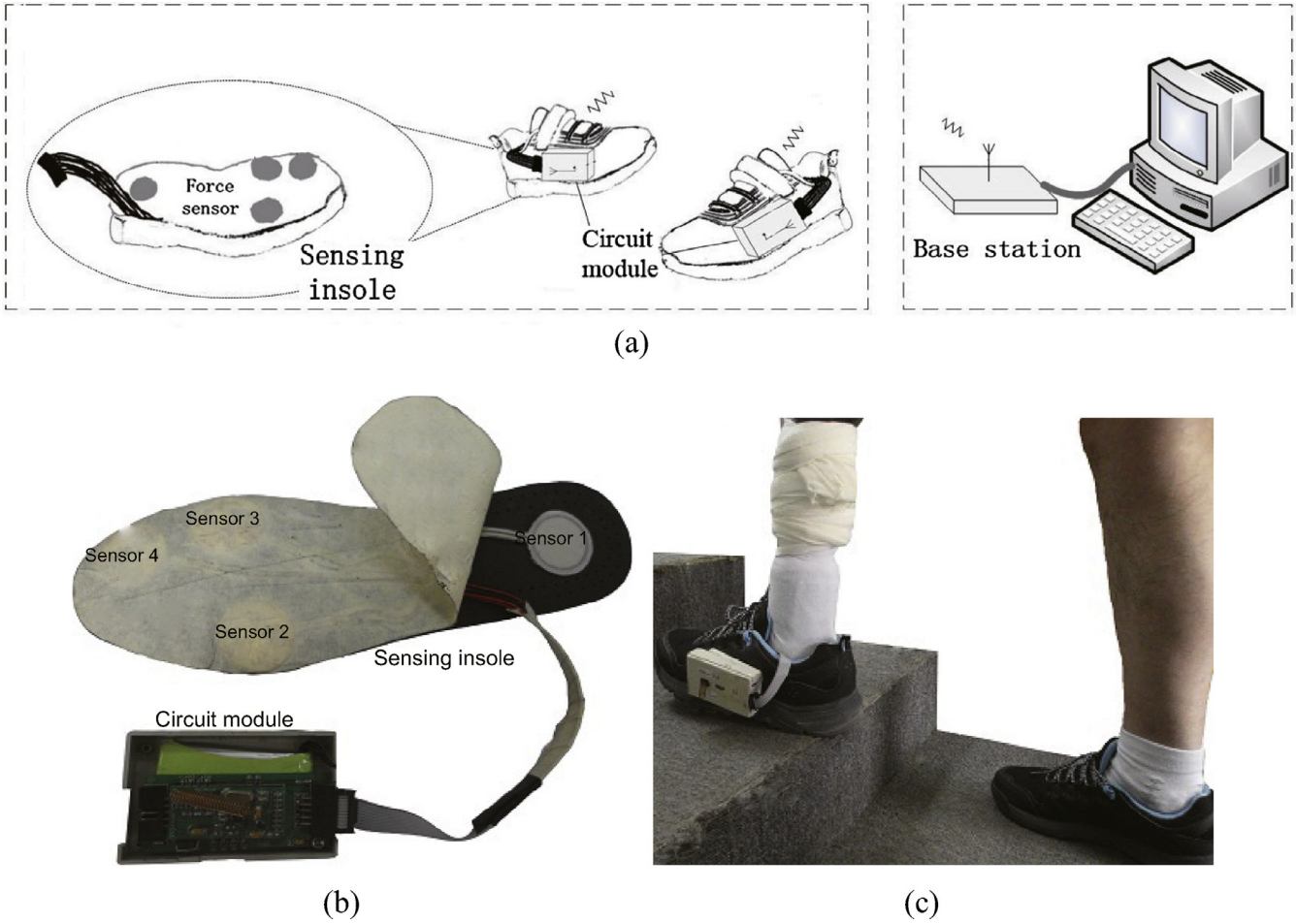

Fig. 1. The discrete contact force measurement system. (a) The system is composed of sensing insoles, circuit modules, and a base station connected to a host computer. (b) The customized sensing insole contains four force sensors planted at selected positions. The circuit module contains the processing circuits and the wireless communication module. (c) The foot-wearable interface is worn by a transtibial amputee subject.

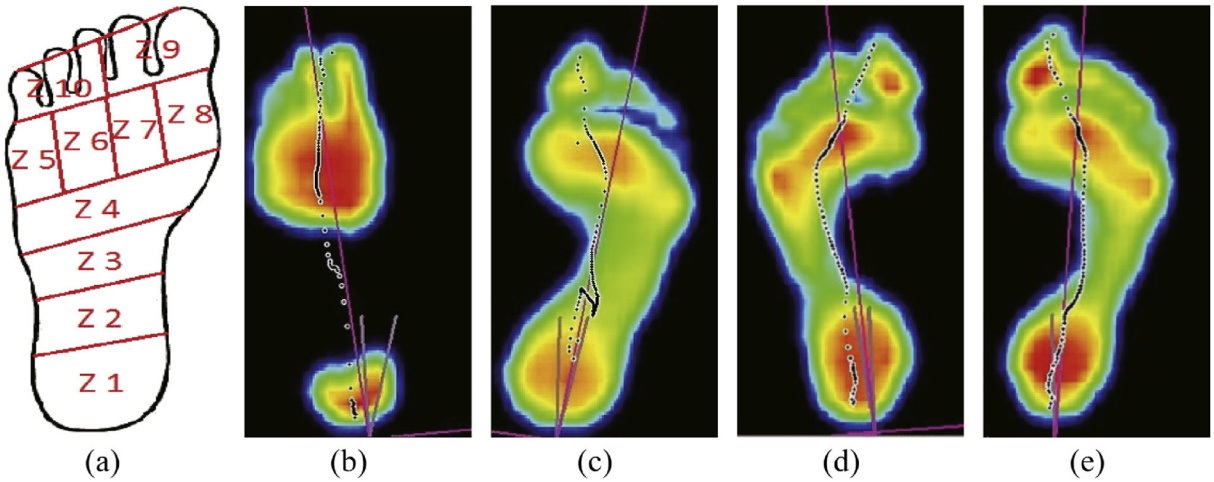

Fig. 2. Sensor placement analysis. (a) The entire contact force distribution area was divided into 10 zones. Contact force signals of both the amputee subject ((b) left prosthetic foot (c) right foot) and able-bodied ((d) left foot, (e) right foot) subjects were measured. Principal component analysis was performed to select the zones which reflected most of the gait information.

while not occupying too much space. Since the force sensors are integrated in the sensing insole, the sensors should be thin enough to avoid uncomfortable sensation. In addition, a simple model is preferred for the conversion from force signals to electrical signals.

According to the above considerations, the *FlexiForce* A401 (Tekscan, Inc.,) force sensor is selected. According to the datasheet, the sensor is 2.08×10^{-4} m thick, and its sensing region is a circle with a 1 inch diameter. The resistance output of the sensor depends

on the loading force. Its response time is less than 5 μs, and the hysteresis is less than 4.5% of full scale.

2.2. Circuits

The circuit module contains two signal process modules and a base station. Each signal process module is placed in a cubic box of size 0.08 m × 0.05 m × 0.02 m weighing 0.076 kg (Fig. 1(c)). It is attached to the lateral surface of a shoe. The signal process module contains a printed circuit board (PCB), a wireless module, and a battery. The PCB has an operational amplifier, an analog to digital (A/D) converter, a microprogrammed control unit (MCU), and a wireless module. When external force is applied on the force sensor, the force signal is converted into an electrical signal with a magnitude proportional to the applied force. Thus, the amplifier outputs an analog voltage proportional to the applied force. The A/D converter then converts the analog voltage to a digital signal and sends the signal to the MCU for processing and encoding. The low-power radio frequency wireless module is used to transmit the data to the computer with 100-Hz sampling frequency. The base station contains a wireless module, an MCU, and a serial line level converter circuit board. The MCU rearranges the data received from the two measurement modules, and then sends the arranged data sequence to the host computer via a serial port.

2.3. Calibration

Force sensors were calibrated with a force generating machine, $AGS-X$ (SHIMADZU, Inc.,). In the calibration experiment, the machine was controlled to generate force ranging from 0 N to 100 N with 10 N increments each time (namely, 0 N, 10 N, 20 N, …, 100 N). In the meantime, output voltage values of the measurement circuit were recorded. In this experiment, no significant hysteresis or response delay were observed.

A linear equation was used to fit the data of force input and voltage output (Fig. 3). The relationship between the voltage output (V_{out}) and the applied force (F_{app}) is

$$V_{out} = 0.0030 \times F_{app} + 1.1109 \quad (1)$$

The residual error of the fitting equation is 0.0114, which means the relationship between the voltage output and the applied force was approximately linear when the loading force was between 0 and 100 N. In this study, force signals measured from all the subjects were below 100 N, within the tested force range in the calibration experiment. Note that the summation of signals measured by sensors on an insole is not the total ground reaction force, as each force sensor can only measure the force applied on its sensing region.

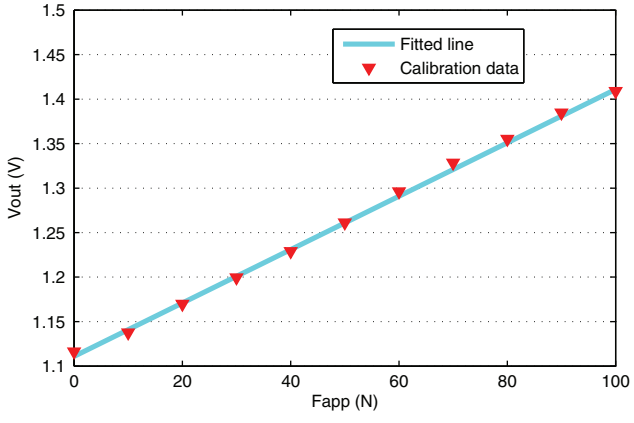

Fig. 3. Calibration data and linear fitted line.

3. Locomotion mode recognition

3.1. Recognition strategy

Human locomotion activities in daily life are usually sequences of repetitive limb movements [34]. As shown in Fig. 4(a), the measured contact force signals are quasi-periodic, and show different characteristics in different gait phases. Similar results are also observed in EMG signals [19] and capacitance signals [21]. Therefore, a phase-dependent classification method [19], which has been used in some previous studies [19,21], is appropriate for the recognition of these repetitive locomotion tasks.

To delimit the continuous data stream by strides, force signals of the four sensors on an insole were summed together (the black curve in Fig. 4(a)), and a threshold detection approach was used to detect foot contact (FC) and foot off (FO) with respect to the ground. FC was defined as the moment when the summed force exceeded a threshold (1/3 of the summed force measured when the subject stands still) and FO is the moment when the summed force dropped below the threshold. In this study, four gait phases are defined by FC and FO:

(a) *Pre-FC*: 0.2 s prior to FC;
(b) *Post-FC*: 0.2 s after FC;
(c) *Pre-FO*: 0.2 s prior to FO;
(d) *Post-FO*: 0.2 s after FO.

In each phase, a 0.2-s analysis window is used for data segmentation and feature extraction. Different gait phases have their own classifiers, which are trained with the data belonging to corresponding phases.

3.2. Classification

3.2.1. Features

Feature values were calculated with the data from the analysis window. Compared to EMG signals and capacitance signals, contact force signals have more explicit physical meanings, which could be helpful for feature extraction.

The feature vector was consisted of three types of feature values. First, as the signal curve of each force sensor appeared in a unique shape for a certain locomotion mode, third-order autoregression coefficients were calculated with the signals segmented by analysis windows to form the first feature sub-vector $\overline{F}_1$. Second, correlation coefficients of signals measured by different sensors in an analysis window reflected temporal relations between different sensing positions, and this information might be useful for the identification of different locomotion modes. Therefore, correlation coefficients of any two force channels of each insole were calculated to form the second feature sub-vector $\overline{F}_2$. Correlation coefficient of channel x and channel y was calculated by

$$r_{xy} = \frac{\sum_{i=1}^{n}(x_i-\bar{x})(y_i-\bar{y})}{\sqrt{\sum_{i=1}^{n}(x_i-\bar{x})^2 \cdot (y_i-\bar{y})^2}}, \quad (2)$$

where n is the number of samples in the analysis window, x_i is the ith sample of channel x and $\bar{x}$ is the mean value of channel x in the window. y_i and $\bar{y}$ are similarly defined. Thirdly, locomotion modes of sitting and standing were different from the others because they were motionless. Contact force signals of these two movement modes usually stayed the same, or slightly varied within a small range. Therefore, variance ranges of all eight channels of

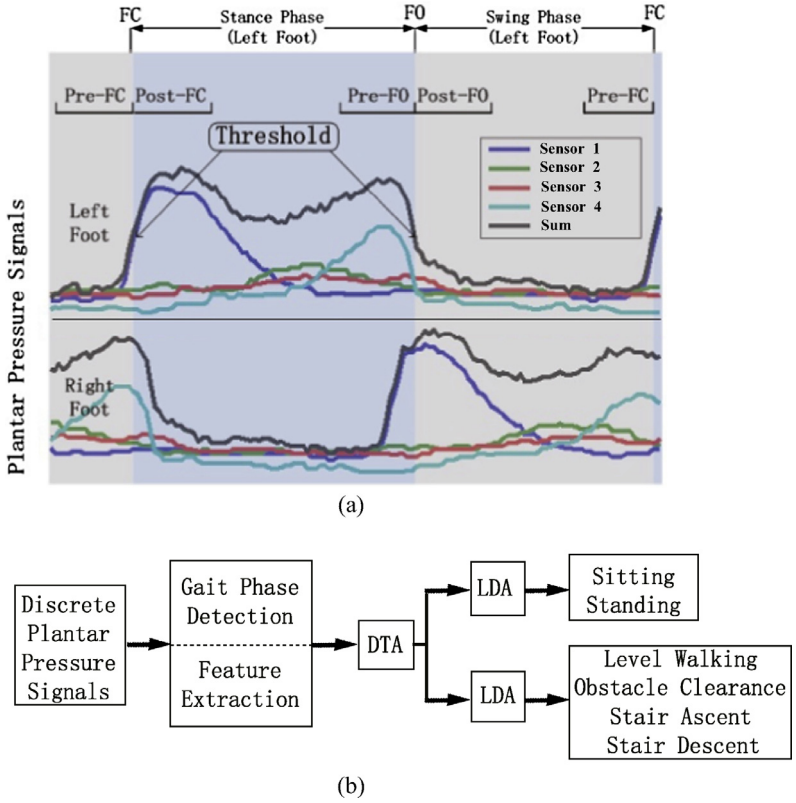

Fig. 4. The illustration of the proposed recognition strategy. (a) A stride of raw signals of an able-bodied subject measured from 4 sensors mounted on each insole. The gait phases are determined by moments that the summed contact force crosses the predefined threshold value. (b) The flow chart of signal processing for locomotion mode recognition.

signals within the analysis window were summed together to form the third feature sub-vector $\overline{F}_3$, which was supposed to provide useful information for separating the motionless locomotion modes to the other modes. Then the feature vector ($\overline{F}$) was formulated as:

$$\overline{F} = \left(\overline{F}_1, \overline{F}_2, \overline{F}_3\right), \tag{3}$$

where $\overline{F}_k$ denotes the kth type of feature sub-vector.

3.2.2. Classifiers

The classification process used was illustrated in Fig. 4(b). First, the summed contact force signals were used for gait phase detection. Then, the measured signals were segmented with corresponding analysis windows and used for feature extraction. Locomotion mode recognition is a two-step procedure. In the first step, a simplified two-branch *decision tree analysis* (DTA) classifier with one decision node was used, whose input is the feature sub-vector $\overline{F}_3$. It was used to determine whether the tested data belonged to the motionless modes (e.g. standing) or the other motion modes (e.g. walking). In the second step, linear discriminant analysis (LDA) classifiers were applied. For both motionless modes and motion modes, they have their own trained classifiers in different phases. Feature sub-vector $\overline{F}_1$ and $\overline{F}_2$ were used to estimate the specified locomotion mode these data belonged to. Please see [35] for details of DTA and LDA.

3.3. Performance evaluation

To make a convincing assessment of the performance for locomotion mode recognition, *K*-fold cross-validation (*K*-CV) was employed. *K*-CV was performed as follows: the entire experiment data were equally divided into *K* folds (each fold should contain data of all tested locomotion tasks). ($K-1$) folds of data were used for classifier training, while the remaining fold used for testing. This procedure was repeated for *K* times, and each fold of the data was used as the testing set for one time. Classifier training and testing were performed individually for each subject.

Quantification of classification performance is represented with recognition accuracy (RA), which is defined as

$$\mathrm{RA} = \frac{N_{\mathrm{cor}}}{N_{\mathrm{total}}} \times 100\%, \tag{4}$$

where N_{cor} denotes the number of correctly classified events, and N_{total} is the total number of tested events.

To understand which modes are prone to be misclassified as some other modes, the confusion matrix is also constructed

$$C = \begin{pmatrix} r_{11} & r_{12} & \dots & r_{1n} \\ r_{21} & r_{22} & \dots & r_{2n} \\ \dots & \dots & \dots & \dots \\ r_{n1} & r_{n2} & \dots & r_{nn} \end{pmatrix}. \tag{5}$$

Each element of the matrix is defined as

$$r_{ij} = \frac{n_{ij}}{n_{i\bullet}} \times 100\%, \tag{6}$$

where n_{ij} represents the number of tested events in mode i while misclassified as mode j. $n_{i\bullet}$ is the total number of tested events in mode i. r_{ij} indicates the rate of targeted mode i estimated as mode j.

4. Experimental results

Three experiments were carried out to verify the feasibility of the proposed foot-wearable interface. The first two experiments were

designed to investigate system stability of long-term working and adaptability to different ground surfaces. The third experiment was performed to evaluate the recognition performance of six locomotion modes for both able-bodied and amputee subjects.

4.1. Stability of long-term working

The proposed 4-position contact force measurement system was designed as a foot-wearable interface for the control of assistive devices such as prosthetic legs and exoskeletons. The output signals of the measurement system were expected to be stable and without time-related drifts after lengthy use. To validate the long-term working stability of the proposed system, an eight-hour experiment was carried out.

In the experiment, an able-bodied subject was recruited and provided written and informed consent. The subject was 24 years old, 75 kg in weight and 1.72 m in height. Signals of the system were measured when the subject was in sitting and standing mode, respectively. In these two motionless modes, contact forces were expected to keep still. Thus, the stability of the measurement system can be reflected by signal variances. In each measurement trial, the subject was firstly asked to sit still for 10 s and contact force signals were recorded. Then the measurement was repeated while the subject was asked to stand still. The measurement trial was performed every 20 min. To evaluate measurement stability after long-term working, the whole experiment lasted for eight hours, and a total of 24 measurement trials were carried out. The subject was allowed to do what he wanted during the interval of two experiment trials.

Experiment results are displayed in Fig. 5. Contact force signals measured from the left foot and the right foot were supposed to be symmetrical for the able-bodied subject. Thus, force signals of only the left foot were analyzed here for simplicity. Mean values and standard deviations of contact force signals measured from *Sensor 1–4* over all the 24 experiment trials were 9.53 ± 0.56, 6.67 ± 0.51, 8.80 ± 0.16, and 3.12 ± 0.28 N for sitting, while 29.10 ± 0.53, 9.64 ± 0.40, 10.24 ± 0.38, and 5.21 ± 0.19 N for standing (see Fig. 5(a)). Average signal variance ratio (the ratio of standard deviation to mean value) was $6.08\% \pm 3.11\%$ and $3.33\% \pm 1.03\%$ for sitting and standing, respectively. In addition, we noticed that the signals measured by the four sensors during sitting and standing have different amplitudes, especially for *Sensor 1*, whose signals measured in standing mode were about three times larger than those in sitting mode. This information is important for the classification of sitting and standing. Fig. 5(a) and (b) shows mean values and standard deviations of *Channel 1–4* signals in each experiment trial of sitting and standing. No obvious signal drift over time was observed for both modes. Results of this experiment indicate that force signals measured by the proposed system were stable, even after the system worked for a relatively long time.

4.2. Adaptability to different ground surfaces

As the proposed interface was integrated with sensing insoles and mounted on shoes, the measured contact force signals might be affected by the ground surface changes. The recognition performance might be therefore influenced. As a consequence, the second experiment was designed to verify the adaptability of the system to different ground surfaces.

Five able-bodied subjects and one unilateral transtibial amputee subject, all free from neurological pathologies, participated in the experiment and provided written and informed consent. The able-bodied subjects had an average age of $23.2(\pm 1.3)$ years, an average weight of $71.4(\pm 8.8)$ kg, an average height of $1.77(\pm 0.03)$ m and an average foot size of $0.265(\pm 0.005)$ m. The amputee subject was 45 years in age, 1.70 m in height, 71.0 kg in weight, and 0.25 m in foot size. In this research, he performed all the experiment tasks with his own passive prosthetic foot (a 0.25-m Otto bock 1S90 foot), which is a type of SACH (solid ankle cushion heel) foot. In this experiment, all the subjects were asked to walk at their preferred speeds across three types of ground surfaces (wood, rubber and carpet). The experiment process is sketched in Fig. 6(a).

Results of contact force measurement when walking on different ground surfaces were investigated. The walkway was prepared to guarantee that contact force signals of an entire stride could be obtained in each type of ground surface. Fig. 6(b)–(d) shows the materials and thickness of the walkway surfaces covered by wood, rubber, and carpet. A total of 15 experiment trials were taken for each subject.

Experiment results of the amputee subject can be found in Fig. 7. Signals measured by different sensors when walking on different ground surfaces are drawn in different colors. The measured contact force signals had similar shapes and consistent tendencies when walking on different ground surfaces for both the prosthetic side and the intact side. Similar results were observed from the measured signals of the five able-bodied subjects. These results indicate that the proposed interface is able to adapt to different ground surfaces.

4.3. Recognition of locomotion modes

The third experiment was designed to evaluate the locomotion mode recognition performance with the proposed interface.

4.3.1. Subjects and measurements

The six subjects recruited in the second experiment also participated in this experiment. The contact force insoles were worn in

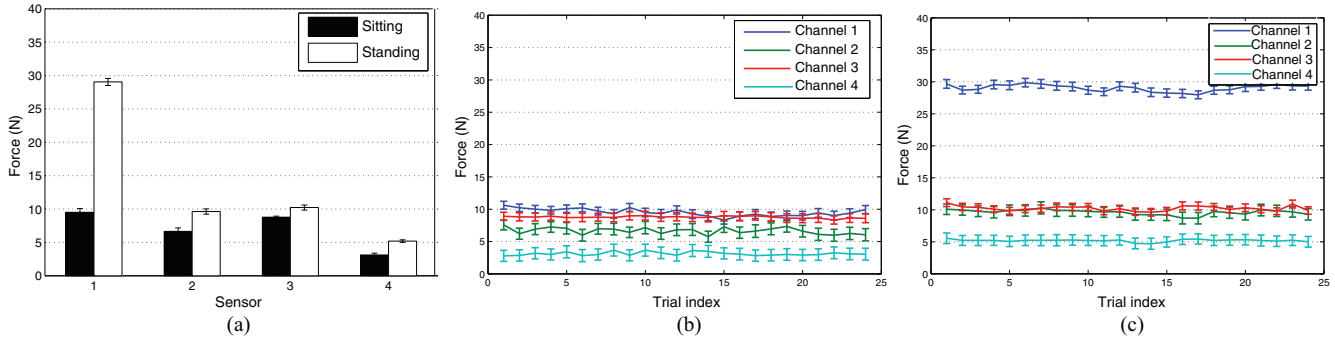

Fig. 5. Signal variation of the proposed system during continuous working on an able-bodied subject. (a) Mean values and standard deviations of contact force signals measured from Sensor 1–4 on the left sensing insole over all the 24 experiment trials for standing and sitting. (b) Mean values and standard deviations of *Channel 1–4* signals in each experiment trial of sitting mode. (c) Mean values and standard deviations of *Channel 1–4* signals in each experiment trial of standing mode.

Fig. 6. (a) Experiment process of walking across different ground surfaces. (b)–(d) The tested ground surfaces.

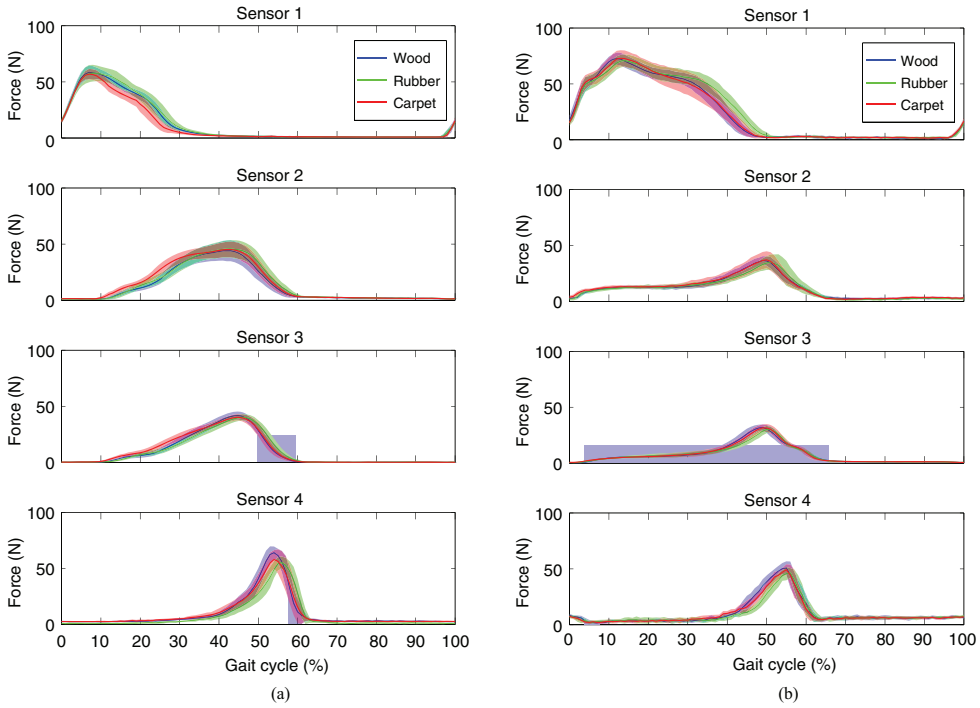

Fig. 7. Contact force signals measured from the amputee subject when walking on different ground surfaces. Signals of a full gait cycle were segmented and averaged over 15 trials. Solid blue, green and red lines denote average contact forces when walking on wood, rubber and carpet, respectively. Color shades denote standard deviations of the measured signals. (a) Signals measured by the sensing insole of the prosthetic side. (b) Signals measured by the sensing insole of the intact side. (For interpretation of the references to color in this figure legend, the reader is referred to the web version of this article.)

both of their shoes, and circuit modules were fixed on the lateral sides of the shoes. The base station was connected to the host computer, and contact force signals were measured at 100 Hz in real time.

4.3.2. Experiment protocol

Six daily-life locomotion modes were investigated, including sitting (SI), standing (ST), level-walking (LW), obstacle clearance (OC), stair ascent (SA), and stair descent (SD). For the task of sitting, the able-bodied subjects were asked to sit on a 0.42-m-high chair while the amputee subject was asked to sit on a 0.65-m-high chair for the convenience of his prosthesis. During standing task, the subjects were required to stand still in each experiment trial. For level-ground walking, the subjects walked at their preferred speeds. Obstacles were 0.40 m wide, 0.18 m deep and 0.25 m high for the able-bodied subjects while 0.40 m wide, 0.25 m deep and 0.18 m high for the amputee subject for safety consideration. The distance between two adjacent obstacles was 0.70 m. The able-bodied subjects were required to alternate their legs to pass over the obstacles. As for the amputee subject, instead of alternatively climbing the obstacles, he stepped over each obstacle with his amputated leg first, followed by the sound leg. This difference is mainly due to safety consideration as well as the amputee's preference. A four-step staircase was used for locomotion tasks of stair ascent and descent. The stairs were 0.75 m in width, 0.40 m in depth and 0.15 m in height. The surface of the staircase was covered by carpet.

In this experiment, the subjects were asked to perform one single type of locomotion task in each trial, and the tested task was repeated for a certain number of times. Contact force signals of different locomotion tasks are shown in Fig. 8, presenting obvious locomotion-dependent signal characteristics. For each locomotion tasks, contact force signals of a total of 150 strides were recorded. The number of experiment trials and stride numbers in each trial for different locomotion tasks are shown in Table 1. For sitting and standing, as no gait events could be detected, strides were manually divided (uniformly distributed along the time) in order to fit in with the classifiers [21]. The subjects were allowed to relax between experiment trials. Before the experiment, some familiarization trials were taken. The subjects were asked to get familiar with the sensing system and the experiment tasks.

4.3.3. Recognition results

K-CV was carried out to evaluate the recognition performance of the proposed foot-wearable interface. We set K to be 5 in this study. Recognition accuracies of different phases were individually calculated. Average recognition accuracies over five able-bodied subjects

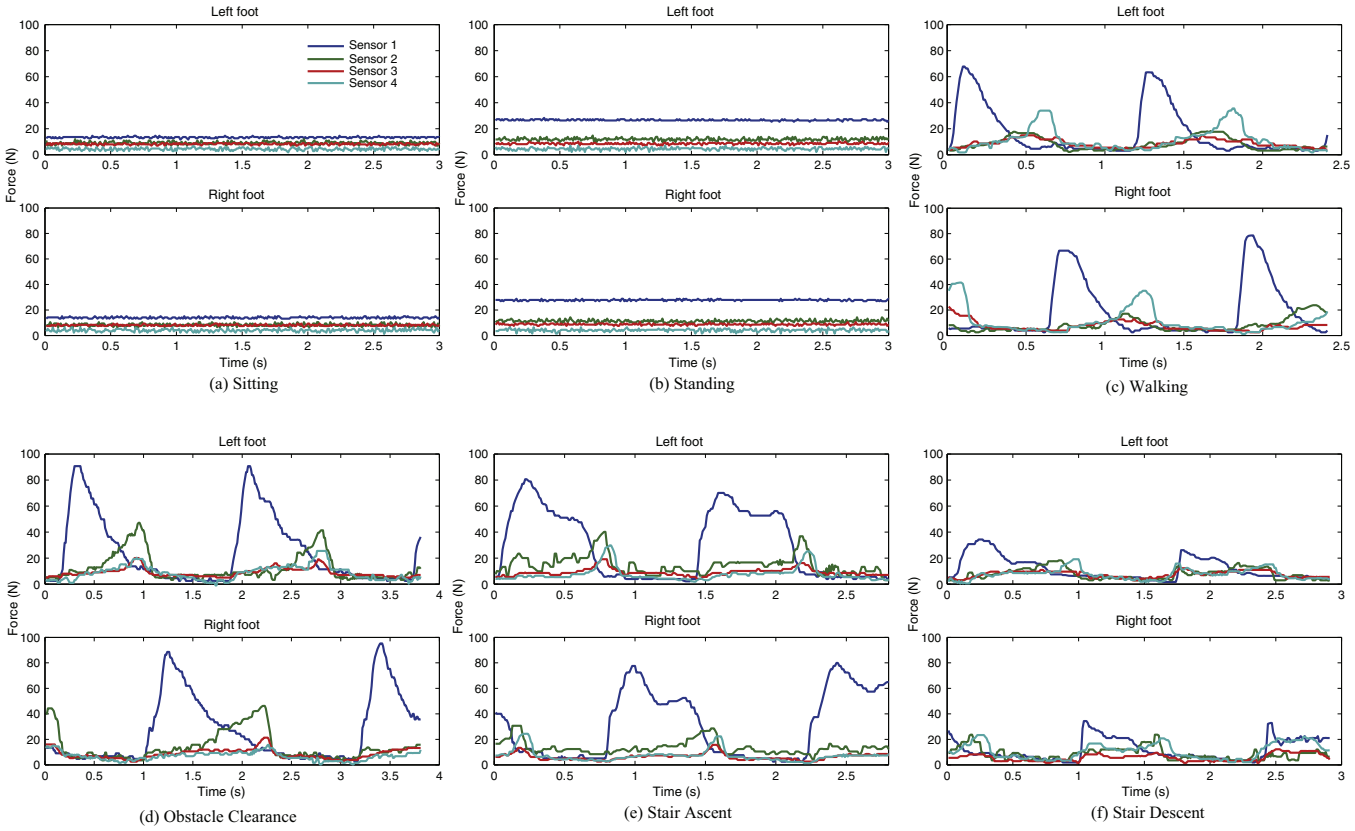

Fig. 8. Discrete contact force signals measured from both feet of an transtibial amputee subject when different locomotion tasks (including sitting, standing, walking, obstacle clearance, stair ascent, and stair descent) were performed. For the modes of walking, obstacle clearance, stair ascent, and stair descent, signals of two entire strides are shown. For sitting and standing modes, 3-s duration of signals are shown.

Table 1
Experimental parameters.

Tasks	Number of trials	Strides per trial	Strides in total
Sitting	10	15	150
Standing	10	15	150
Level-walking	30	5	150
Obstacles clearance	30	5	150
Stair ascent	75	2	150
Stair descent	75	2	150

were $99.2\% \pm 0.4\%$, $99.1\% \pm 0.5\%$, $98.9\% \pm 0.6\%$, and $97.9\% \pm 0.7\%$ for Pre-FC, Post-FC, Pre-FO, and Post-FO, respectively. Recognition accuracies of the amputee subject were 99.1%, 99.0%, 98.6%, and 96.8% for the four corresponding phases. The overall recognition accuracy of able-bodied subjects ($98.8\% \pm 0.5\%$) and the amputee subject (98.4%) were similar. Detailed classification results represented by confusion matrices are shown in Tables 2 and 3.

The best recognition performance with the foot-wearable interface was observed in the classification of sitting and standing (nearly 100% recognition accuracy) for both able-bodied and amputee subjects. As mentioned above, sitting and standing are motionless modes, and the measured signals are almost time-invariant, which is different from the other investigated locomotion modes. We obtained better recognition performance in these two modes than the others, probably due to utilization of the feature subvector $\bar{F}_3$ and DTA classier. Post-FO was the phase with the lowest average recognition accuracy, and most classification errors were caused by the confusion of OC, SA, and SD. When the foot left the ground during these three locomotion tasks, the push-off force in the forward–backward direction was smaller than that during walking, as the body's mass center had smaller forward velocity. That may explain why these three locomotion modes were more easily confused than LW.

4.4. Discussion

In this study, we intended to explore whether discrete contact force distribution could provide valuable information for locomotion mode recognition. As we know, plantar pressure distribution contains rich human gait information. However, only a few studies have applied wearable plantar pressure measurement systems (e.g. sensing insoles) for the control of robotic assistive devices, and most of them used the measured contact force signals for gait phase detection (e.g. [4]). Therefore, we aimed to explore other potential application spaces (e.g. locomotion mode recognition) of plantar pressure signals for wearable assistive robot control. In this research, two 4-position sensing insoles were used for measuring contact force signals. With phase-dependent recognition strategy, six locomotion tasks were investigated and obtained satisfactory overall recognition performance (recognition accuracy was 98.8% for able-bodied subjects and 98.4% for the amputee subject). The recognition performance is comparable with those achieved using EMG signals (average classification accuracy was 92.2% for able-bodied subjects and 91.6% for amputee subjects [19]) and capacitance signals (average classification accuracy was 93.6% for able-bodied subjects and 93.4% for amputee subjects [21]). The results indicate that the foot-wearable interface based on discrete contact force distribution does provide valuable information for locomotion mode recognition.

Compared with other sensing systems (e.g. EMG) used for locomotion mode recognition, the proposed foot-wearable interface has the following advantages. First, the interface is wearable and easy

Table 2
Confusion matrix (mean ± SEM (standard error of the mean)) for able-bodied subjects (%).

Phase	Targeted mode	Estimated mode					
		SI	ST	LW	OC	SA	SD
Pre-FC	SI	100.0 ± 0.0	0.0 ± 0.0	0.0 ± 0.0	0.0 ± 0.0	0.0 ± 0.0	0.0 ± 0.0
	ST	0.0 ± 0.0	99.8 ± 0.2	0.0 ± 0.0	0.0 ± 0.0	0.2 ± 0.2	0.0 ± 0.0
	LW	0.0 ± 0.0	0.0 ± 0.0	99.7 ± 0.3	0.3 ± 0.3	0.0 ± 0.0	0.0 ± 0.0
	OC	0.0 ± 0.0	0.0 ± 0.0	0.5 ± 0.3	97.7 ± 0.5	1.5 ± 0.8	0.3 ± 0.3
	SA	0.0 ± 0.0	0.2 ± 0.2	0.0 ± 0.0	0.5 ± 0.5	99.1 ± 0.9	0.2 ± 0.2
	SD	0.0 ± 0.0	0.0 ± 0.0	0.0 ± 0.0	0.0 ± 0.0	1.2 ± 0.5	98.9 ± 0.5
Post-FC	SI	100.0 ± 0.0	0.0 ± 0.0	0.0 ± 0.0	0.0 ± 0.0	0.0 ± 0.0	0.0 ± 0.0
	ST	0.0 ± 0.0	100.0 ± 0.0	0.0 ± 0.0	0.0 ± 0.0	0.0 ± 0.0	0.0 ± 0.0
	LW	0.0 ± 0.0	0.0 ± 0.0	97.2 ± 0.9	1.4 ± 1.4	1.4 ± 0.5	0.0 ± 0.0
	OC	0.0 ± 0.0	0.0 ± 0.0	0.0 ± 0.0	98.8 ± 0.4	1.0 ± 0.4	0.2 ± 0.2
	SA	0.0 ± 0.0	0.0 ± 0.0	0.2 ± 0.2	0.4 ± 0.3	99.4 ± 0.2	0.0 ± 0.0
	SD	0.0 ± 0.0	0.0 ± 0.0	0.0 ± 0.0	0.0 ± 0.0	1.2 ± 0.5	98.9 ± 0.5
Pre-FO	SI	100.0 ± 0.0	0.0 ± 0.0	0.0 ± 0.0	0.0 ± 0.0	0.0 ± 0.0	0.0 ± 0.0
	ST	0.0 ± 0.0	100.0 ± 0.0	0.0 ± 0.0	0.0 ± 0.0	0.0 ± 0.0	0.0 ± 0.0
	LW	0.0 ± 0.0	0.0 ± 0.0	99.1 ± 2.3	0.5 ± 0.5	0.0 ± 0.0	0.4 ± 0.4
	OC	0.0 ± 0.0	0.0 ± 0.0	0.0 ± 0.0	99.6 ± 0.3	0.2 ± 0.2	0.3 ± 0.3
	SA	0.0 ± 0.0	0.0 ± 0.0	0.2 ± 0.2	0.9 ± 0.6	98.2 ± 1.0	0.7 ± 0.4
	SD	0.0 ± 0.0	0.0 ± 0.0	0.2 ± 0.2	0.6 ± 0.4	2.9 ± 1.9	96.2 ± 2.0
Post-FO	SI	99.2 ± 0.4	0.0 ± 0.0	0.0 ± 0.0	0.0 ± 0.0	0.5 ± 0.5	0.4 ± 0.2
	ST	0.0 ± 0.0	99.6 ± 0.2	0.0 ± 0.0	0.2 ± 0.2	0.2 ± 0.2	0.0 ± 0.0
	LW	0.0 ± 0.0	0.0 ± 0.0	99.0 ± 0.6	1.0 ± 0.6	0.0 ± 0.2	0.0 ± 0.0
	OC	0.2 ± 0.2	0.3 ± 0.3	1.2 ± 0.8	95.5 ± 1.1	1.8 ± 0.9	1.1 ± 0.8
	SA	0.0 ± 0.0	0.0 ± 0.0	0.0 ± 0.0	1.3 ± 0.6	97.4 ± 1.3	1.3 ± 0.8
	SD	0.5 ± 0.5	0.2 ± 0.2	0.0 ± 0.0	0.4 ± 0.2	2.4 ± 1.0	96.5 ± 1.3

Table 3
Confusion matrix for the amputee subject (%).

Phase	Targeted mode	Estimated mode					
		SI	ST	LW	OC	SA	SD
Pre-FC	SI	100.0	0.0	0.0	0.0	0.0	0.0
	ST	0.0	100.0	0.0	0.0	0.0	0.0
	LW	0.0	0.0	100.0	0.0	0.0	0.0
	OC	0.0	0.0	0.0	96.3	0.0	3.7
	SA	0.0	0.0	0.0	0.0	100.0	0.0
	SD	0.0	0.0	0.0	2.0	0.0	98.0
Post-FC	SI	100.0	0.0	0.0	0.0	0.0	0.0
	ST	0.0	100.0	0.0	0.0	0.0	0.0
	LW	0.0	0.0	100.0	0.0	0.0	0.0
	OC	0.9	0.0	3.7	95.4	0.0	0.0
	SA	0.0	0.0	0.7	0.0	99.3	0.0
	SD	0.0	0.0	0.0	0.7	0.0	99.3
Pre-FO	SI	100.0	0.0	0.0	0.0	0.0	0.0
	ST	0.0	100.0	0.0	0.0	0.0	0.0
	LW	0.0	0.0	95.1	1.2	3.1	0.6
	OC	0.0	0.0	0.9	98.2	0.9	0.0
	SA	0.0	0.0	0.0	0.0	99.3	0.7
	SD	0.0	0.0	0.0	0.0	0.7	99.3
Post-FO	SI	100.0	0.0	0.0	0.0	0.0	0.0
	ST	0.0	100.0	0.0	0.0	0.0	0.0
	LW	0.0	0.0	98.6	0.0	1.4	0.0
	OC	0.0	0.0	2.7	97.3	0.0	0.0
	SA	0.0	0.0	0.7	0.0	93.9	5.5
	SD	0.0	0.0	1.4	0.0	7.4	91.2

to integrate with existing robotic assistive devices. The sensing insoles have thin force sensors and can be easily placed in users' shoes without causing discomfort. The circuit modules are designed to be lightweight, small and friendly wearable, and they can be attached to the lateral surfaces of users' shoes. Wireless communication makes it easier to integrate with various robotic assistive devices. Second, the foot-wearable interface has stable signal measurement performance during long-term working, which is important for a recognition system. Therefore, deterioration of recognition accuracy over time caused by signal variation (e.g. EMG signals, see [36]) will not be a problem for the proposed system.

Unlike the commercially available pressure insoles with high sensor distribution density, the presented contact force measurement system has only four sensors on each insole. Insoles with more force sensors can certainly provide more detailed plantar pressure distribution information. However, computation burden also greatly increases. As the proposed system aims for robotic device control, timeliness is an important factor to consider. Therefore, the insole should collect most of the useful information with as few sensors as possible. PCA is performed to investigate this issue, and four positions are selected for sensor placement, which include zones under the calcaneus tuberosity, the fourth metatarsal, the first metatarsal, and the hallux.

Though the foot-wearable interface has the advantages mentioned above, it still has some deficiencies for locomotion mode recognition. First, compared with intact feet, prosthetic feet have flatter plantar surfaces and some of them have no ankle joints or toe joints. Therefore, the measured contact force signals of prosthetic feet contain relatively less useful information. It may be the reason why the overall recognition accuracy of able-bodied subjects is a little higher than that of the amputee subject. Second, when wearers walk on uneven terrains or places with small holes, some parts of their shoes may not fully contact with the ground, and some useful information may be not included in the measured force signals. In addition, locomotion information collected by the proposed system is still limited, and recognition performance with the interface alone is not sufficient for assistive device control. Therefore, the presented system should be combined with other sensing systems to achieve better recognition performance (more tested locomotion tasks and higher classification accuracy).

5. Conclusion

In this paper, we aim to explore the potential of using signals of discrete contact force distribution for human locomotion mode recognition. The presented measurement system shows stable measurement performance during long term working conditions with no time-related signal drifts. No obvious difference is observed in the measured signals when walking on different ground surfaces. With the phase-dependent recognition strategy, LDA and DTA are used to recognize six locomotion tasks and achieve satisfactory recognition performance for both amputee and able-bodied subjects. These results indicate that the proposed foot-wearable interface can provide useful information for human locomotion mode recognition and could be a supplementary for existing recognition systems to achieve improved classification performance. In our future work, we will combine the proposed interface with other sensing systems (e.g. EMG and mechanical sensors) to realize continuous recognition throughout the locomotion period (including locomotion transitions), and more locomotion tasks will be investigated. The system will also be integrated with robotic assistive systems, and its potential for clinical application will be investigated.

Acknowledgments

This work was supported by the National Natural Science Foundation of China (Nos. 61005082 and 61020106005), the Beijing Nova Program (No. Z141101001814001), the Beijing Municipal Science and Technology Project (No. Z151100003715001), the PKU-Biomedical Engineering Joint Seed Grant 2014 and the 985 Project of Peking University (No. 3J0865600). We would like to thank the anonymous reviewers for their valuable suggestions that improved this article.

References

[1] Bamberg SJM, Benbasat AY, Scarborough DM, Krebs DE, Paradiso JA. Gait analysis using a shoe-integrated wireless sensor system. IEEE Trans Inf Technol B 2008;12:413–23.
[2] Tekscan. Tactile pressure measurement, pressure mapping systems, force sensors and measurement systems <http://www.tekscan.com/>.
[3] Novel quality in measurement <http://www.novel.de/>.
[4] Pappas I, Popovic M, Keller T, Dietz V, Morari M. A reliable gait phase detection system. Trans Neural Syst Rehab Eng 2001;9:113–25.
[5] Carrozza MC, Persichetti A, Laschi C, Vecchi F, Lazzarini R, Vacalebri P, et al. A wearable biomechatronic interface for controlling robots with voluntary foot movements. IEEE/ASME Trans Mechatron 2007;12:1–11.
[6] Chen M, Huang B, Xu Y. Intelligent shoes for abnormal gait detection. In: Proceedings of the IEEE international conference on robotics and automation; 2008. p. 2019–24.
[7] Kong K, Tomizuka M. A gait monitoring system based on air pressure sensors embedded in a shoe. IEEE/ASME Trans Mechatron 2009;14:358–70.
[8] Shu L, Hua T, Wang Y, Li Q, Feng DD, Tao X. In-shoe plantar pressure measurement and analysis system based on fabric pressure sensing array. IEEE Trans Inf Technol B 2010;14:767–75.
[9] Holleczek T, Ruegg A, Harms H, Troster G. Textile pressure sensors for sports applications. In Proceeding of IEEE sensors; 2010. p. 732–7.
[10] Sazonov ES, Fulk G, Hill J, Schutz Y, Browning R. Monitoring of posture allocations and activities by a shoe-based wearable sensor. IEEE Trans Biomed Eng 2011;58:983–90.
[11] Saito M, Nakajima K, Takano C, Ohta Y, Sugimoto C, Ezoe R, et al. An in-shoe device to measure plantar pressure during daily human activity. Med Eng Phys 2011;33:638–45.
[12] Healy A, Burgess-Walker P, Naemi R, Chockalingam N. Repeatability of WalkinSense in shoe pressure measurement system: a preliminary study. Foot 2012;22:35–9.
[13] Donati M, Vitiello N, De Rossi SMM, Lenzi T, Crea S, Persichetti A, et al. A flexible sensor technology for the distributed measurement of interaction pressure. Sensors 2013;13:1021–45.
[14] Au S, Berniker M, Herr H. Powered ankle–foot prosthesis to assist level-ground and stair-descent gaits. Neural Netw 2008;21:654–66.
[15] Sup F, Varol HA, Goldfarb M. Upslope walking with a powered knee and ankle prosthesis: initial results with an amputee subject. IEEE Trans Neural Syst Rehab Eng 2011;19:71–8.
[16] Yuan K, Zhu J, Wang Q, Wang L. Finite-state control of powered below-knee prosthesis with ankle and toe. In: Proceedings of the 18th world congress of the international federation of automatic control; 2011. p. 2865–70.
[17] Peeraer L, Aeyels B, Van Der Perre G. Development of EMG-based mode and intent recognition algorithms for a computer-controlled above-knee prosthesis. J Biomed Eng 1990;12:178–82.
[18] Ha KH, Varol HA, Goldfarb M. Volitional control of a prosthetic knee using surface electromyography. IEEE Trans Biomed Eng 2011;58:144–51.
[19] Huang H, Kuiken TA, Lipschutz RD. A strategy for identifying locomotion modes using surface electromyography. IEEE Trans Biomed Eng 2009;56:65–73.
[20] Cheng J, Amft O, Lukowicz P. Active capacitive sensing: exploring a new wearable sensing modality for activity recognition. In: Pervasive Computing, LNCS, vol. 6030; 2010. p. 319–36.
[21] Chen B, Zheng E, Fan X, Liang T, Wang Q, Wei K, et al. Locomotion mode classification using a wearable capacitive sensing system. IEEE Trans Neur Sys Rehab Eng 2013;21(5):744–55.
[22] Varol HA, Sup F, Goldfarb M. Multiclass real-time intent recognition of a powered lower limb prosthesis. IEEE Trans Biomed Eng 2010;57:542–51.
[23] Young A, Simon A, Hargrove L. A training method for locomotion mode prediction using powered lower limb prostheses. IEEE Trans Neur Sys Rehab Eng 2014;22(3):671–7.
[24] Yuan K, Wang Q, Wang L. Fuzzy-logic-based terrain identification with multisensor fusion for transtibial amputees. IEEE/ASME Trans Mechatron 2015;20(2):618–30.
[25] Huang H, Zhang F, Hargrove L, Dou Z, Rogers D, Englehart K. Continuous locomotion mode identification for prosthetic legs based on neuromuscular-mechanical fusion. IEEE Trans Biomed Eng 2011;58:2867–75.
[26] Au SK, Weber J, Herr H. Powered ankle–foot prosthesis improves walking metabolic economy. IEEE Trans Robot 2009;25:51–66.
[27] Lawson B, Varol HA, Goldfarb M. Standing stability enhancement with an intelligent powered transfemoral prosthesis. IEEE Trans Biomed Eng 2011;58:2617–24.
[28] Zhu J, Wang Q, Wang L. On the design of a powered transtibial prosthesis with stiffness adaptable ankle and toe joints. IEEE Trans Ind Electr 2014;61:4797–807.
[29] Li Y, Becker A, Shorter KA, Bretl T, Hsiao-Wecksler ET. Estimating system state during human walking with a powered ankle–foot orthosis. IEEE/ASME Trans Mechatron 2011;16(5):835–44.
[30] Shorter KA, Kogler GF, Loth E, Durfee WK, Hsiao-Wecksler ET. A portable powered ankle–foot-orthosis for rehabilitation. J Rehabil Res Dev 2011;48(4):459–72.
[31] Li Y, Hsiao-Wecksler ET, Gait mode recognition and control for a portable-powered ankle–foot orthosis. In: Proceedings of the 13th international conference on rehabilitation robotics; 2013. p. 1–8.
[32] Orlin M, McPoil T. Plantar pressure assessment. Phys Therapy 2000;80:399–409.
[33] Wen J, Ding Q, Yu Z, Sun W, Wang Q, Wei K. Adaptive changes of foot pressure in hallux valgus patients. Gait Post 2012;36:344–9.
[34] Perry J. Gait analysis. Thorofare (NJ): SLACK, Inc.,; 1992.
[35] Hastie T, Tibshirani R, Friedman J, Hastie T, Friedman J, Tibshirani R. The elements of statistical learning. New York: Springer; 2009.
[36] Jain S, Singhal G, Smith RJ, Kaliki R, Thakor N. Improving long term myoelectric decoding, using an adaptive classifier with label correction. In: Proceedings of the 4th IEEE RAS and EMBS international conference on biomedical robotics and biomechatronics; 2012. p. 532–7.